



<b>Experiment title:</b> X-ray Fluorescence microscopy study of cation distribution in AD tissue: colocalization with amyloid plaques and lipid oxidation determined by Infrared Microscopy	<b>Experiment number:</b> LS-2499
<b>Beamline:</b> ID21 and ID16B-NA	<b>Date of experiment:</b> from: 02/03/2016 to: 08/03/2016 and from: 11/07/2016 to: 15/07/2016
<b>Shifts:</b> 18	<b>Local contact(s):</b> Hiram CASTILLO-MICHEL (in ID21) and Vanessa Isabel TARDILLO SUAREZ (in ID16B)
<b>Date of report:</b> September, 2016  <i>Received at ESRF:</i>	

**Names and affiliations of applicants** (\* indicates experimentalists):

Núria Benseny-Cases\*<sup>1</sup>, Hiram Castillo-Michel\*<sup>2</sup>, Ester Aso<sup>3</sup>, Isidro Ferrer<sup>3</sup>, Josep Cladera\*<sup>4</sup>, Elena Álvarez-Marimon\*<sup>4</sup>

<sup>1</sup> Laboratory ALBA-CELLS, Bellaterra ES - 08193, Barcelona, Spain

<sup>2</sup> Laboratory ESRF 71 avenue des Martyrs CS 40220 FR - 38043 Grenoble, France

<sup>3</sup> Laboratory Institut de Neuropatologia Servei Anatomia Patològica, IDIBELL - Hospital Universitari de Bellvitge Carrer Feixa Llarga sn ES - 08907 Hospitalet de Llobregat, Spain

<sup>4</sup> Laboratory Universidad Autonoma de Barcelona Centre Estudis en Biofísica - CEB Facultat de Medicina Bellaterra ES – 08193 Barcelona, Spain

**Report:**

**Summary:** In the present study, the combined use of synchrotron radiation-based  $\mu$ XRF and  $\mu$ FTIR techniques made possible to relate the severity of Alzheimer Disease (AD) dementia with characteristic secondary structures of A $\beta$  amyloid peptide, elevated levels of metal ions (Cu, Zn, Fe, Ca) and lipid oxidation. The oxidation measurements are in agreement with previous studies (1, 2) and we now relate them with increased levels of metal cations. Most interestingly, the infrared analysis using Principal Component Analysis (PCA) has made possible for the first time the distinction of two types of amyloid aggregates on human cortex samples absorbing at  $1625\text{ cm}^{-1}$  or  $1630\text{-}35\text{ cm}^{-1}$  (fig. 2) which might correspond to dense core plaques and diffuse plaques respectively. In addition, we have found a correlation between the type of aggregate and the different metal levels in the different AD stages. This differentiation between two kinds of aggregates, highly relevant in AD because it is related to amyloid toxicity, is shown for the first time in an ‘in situ’ human cortex tissue analysis for AD amyloid deposits which has been only reported once before for Huntington disease amyloid inclusion bodies (3).

**Methodology:** cryosectioned and cryo-dried human brain tissue samples were cut in contiguous slides of  $8\text{ }\mu\text{m}$  thick of the cortex region affected by AD. Age-related brain tissue of nonaffected by AD of corresponding cortices were taken as a control. The senile plaques were localized by use of the fluorescent dye Thioflavin S (ThS), which becomes fluorescent when combining with aggregates. Then contiguous slices of the same region were mounted on  $\text{Si}_3\text{N}_4$  windows suitable for  $\mu$ XRF and  $\mu$ FTIR analyses. The  $\mu$ FTIR map of Senile Plaques and the tissue surrounding the plaques was measured with a  $10\times 10\text{ }\mu\text{m}^2$   $\mu$ FTIR beam, step size  $5\text{ }\mu\text{m}$  and 128 scans at each pixel. Spectra was acquired over the  $700\text{-}4000\text{ cm}^{-1}$  region using the MCT-B detector. For  $\mu$ XRF imaging at ID21 the energy was fixed at  $7.2\text{ keV}$  close to the Fe K-edge and maps of  $2\text{ }\mu\text{m}^2$  pixel size were obtained from big areas. At ID16 the energy was fixed at  $17.5\text{ keV}$ , so we could analyze Cu and Zn in the same samples at  $0.15\text{ }\mu\text{m}^2$  pixel size. The strategy followed was first to map the amyloid deposits of AD tissue cortice slides by FTIR imaging at ID21, and then, the same regions were analyzed for metals by  $\mu$ XRF at ID21 and ID16B beam lines. Maps at ID16B were taken at different zones from ID21 to avoid analyzing damage irradiation regions. A python script to transfer coordinates through references from the optical images allowed to easily localize the same areas (fig. 1). Data was analyzed using OMNIC, PyMCA programs, and PCA was used for the statistical analysis (Unscramble).

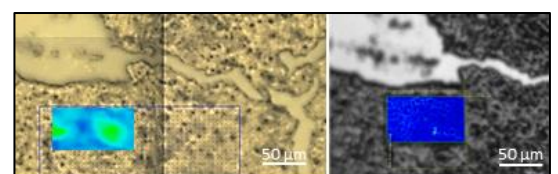


**Figure 1.**  $\mu$ FTIR and  $\mu$ XRF optical images of same regions mapped.

**Results:** In agreement with previous results (2) the FTIR imaging data shows that there is a colocalization of the amyloid aggregates with oxidized lipid in the plaques themselves and in the tissue immediately surrounding the aggregates. A deeper analysis of the infrared data has been carried out using Principal Component Analysis (PCA) showing a clear distinction in the analysed tissues of two different types of amyloid aggregates absorbing at  $1625\text{ cm}^{-1}$  and at  $1630\text{-}35\text{ cm}^{-1}$  (fig. 2). This is being shown for the first time in an ‘in situ’ human tissue analysis for AD amyloid deposits and it has been only reported once before for Huntington disease amyloid inclusion bodies (3). The distinction between amyloid aggregates is a central point in relation to amyloid toxicity since toxicity is related to the formation of aggregates (oligomers, amorphous aggregates) structurally distinct from amyloid fibrils. Such a distinction has been largely explored in ‘in vitro’ studies of the amyloid oligomerization process, but is the first time found ‘in situ’ in human tissue.

The  $\mu$ XRF results show that Fe, Cu, Zn and Ca ion maps co-localize with the plaques and their surroundings with a cation content in these regions well above the level measured in the controls (fig. 2d-e). This is in agreement with previous reports by the group of Lisa Miller (4) on human and transgenic mouse tissue. Cu and Zn show the same pattern distribution in all cases. For Ca, it is shown to increase at stage VI, and it co-localizes well with Cu and Zn. Moreover, the analysis of the  $\mu$ XRF maps reveals that there are clear differences in the level of metal cations between tissue containing ‘low frequency aggregates’ (peptide aggregates absorbing at  $1625\text{ cm}^{-1}$  in the infrared) and ‘high frequency aggregates’ (peptide aggregates absorbing at  $1630\text{-}35\text{ cm}^{-1}$  in the infrared). For example, in Cu and Zn maps it can clearly be seen that tissue samples from an ADV patient with ‘high frequency’ amyloid aggregates show cation levels similar to those of the controls, whereas samples from ADV and ADVI patients with ‘low frequency’ amyloid aggregates show cation levels well above the controls.

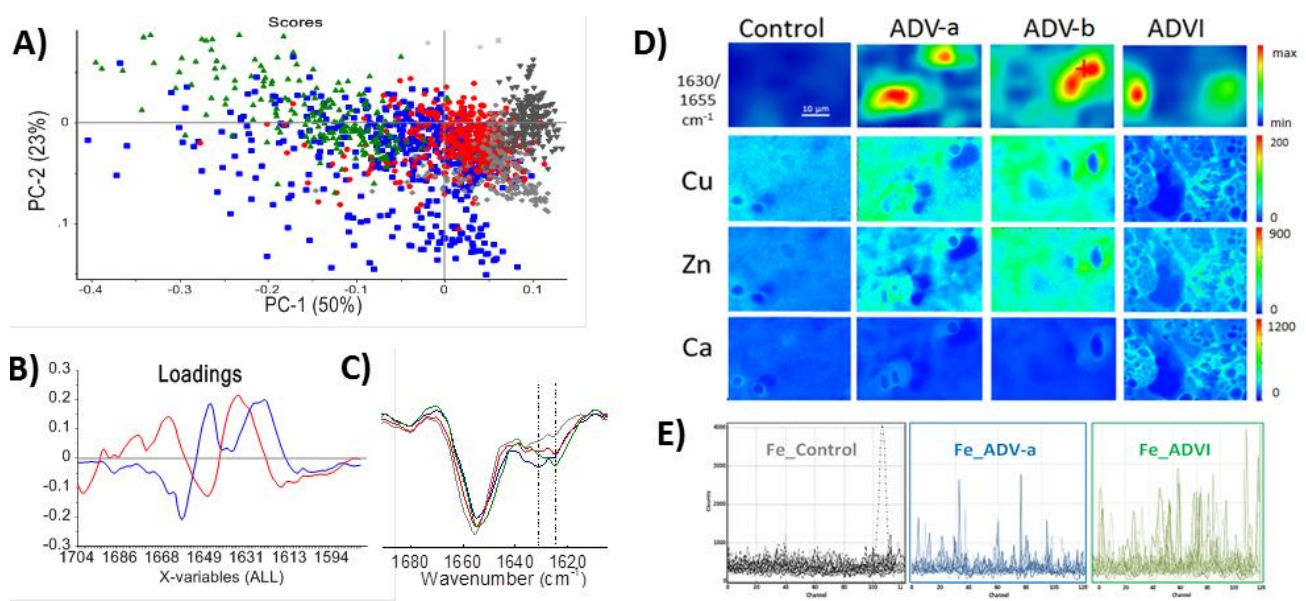


**Figure 2.** **A)** PCA analysis of the Amida I. (3 different controls in different greys, ADVI in green, ADV-a (patient ‘a’) in blue and ADV-b (patient ‘b’) in red) **B)** PCA loadings (PC1 in black and PC2 in grey). **C)** FTIR spectra of the different aggregates (controls in grey, ADVI in green, ADV-a in blue and ADV-b in red). **D)**  $\mu$ FTIR and  $\mu$ XRF maps of a healthy control, ADV-a, ADV-b and AD stage VI tissue sections are shown. In the first row,  $\mu$ FTIR maps of  $1630/1655\text{ cm}^{-1}$  ratio show the aggregates in red. Next rows correspond to  $\mu$ XRF of Cu, Zn, Ca. For all maps intensities were normalized and expressed as red – maximum (214 Cu cps, 914 Zn cps, 1300 Ca cps) and blue – minimum (0 Cu, Zn and Ca cps). **E)** Metal ion analysis. Fe maps of Control, ADV and AD VI samples were analyzed by lines (rows and columns) and shown as counts per channel. **A higher content in metal ion associated to amyloid plaques is detected for samples containing a higher content in ‘low frequency amyloid aggregates’ (peptide aggregates absorbing at  $1625\text{ cm}^{-1}$  in the infrared).**

From our study, the combination of the two techniques ( $\mu$ FTIR and  $\mu$ XRF), has made possible establishing a new link between amyloid deposits, tissue oxidation and elevated metal cation levels ‘in situ’ for the first time. Because the relationship between structurally distinguishable amyloid aggregates, tissue oxidation and metal ion levels is of high significance in AD research, the results from experiments in ESRF’ lines ID21 and ID16B are of great scientific value.

## References

- [1] Ferrer I. Prog Neurobiol 2012 Apr 97(1):38-51  
 [2] Benseny-Cases N. et al. Anal Chem 2014, Dec 16;86(24):12047-5  
 [3] André W et al. Anal Chem 2013 Apr 2;85(7):3765-73  
 [4] Miller LM et al. J Struct Biol 2006 Jul;155(1):30-37